Quantitative MRFM characterization of the autonomous and forced dynamics in a spin transfer nano-oscillator

A. Hamadeh, Grégoire De Loubens, V. V. Naletov, J. Grollier, Ch. Ulysse, V. Cros, O. Klein

HAL Id: hal-00664531
https://hal.archives-ouvertes.fr/hal-00664531

Quantitative MRFM characterization of the autonomous and forced dynamics in a spin transfer nano-oscillator

A. Hamadeh,[1] G. de Loubens,[1, *] V.V. Naletov,[1, 2] J. Grollier,[3] C. Ulysse,[4] V. Cros,[3] and O. Klein[1, †]

[1]*Service de Physique de l'État Condensé (CNRS URA 2464), CEA Saclay, 91191 Gif-sur-Yvette, France*
[2]*Physics Department, Kazan Federal University, Kazan 420008, Russian Federation*
[3]*Unité Mixte de Physique CNRS/Thales and Université Paris Sud 11, RD 128, 91767 Palaiseau, France*
[4]*Laboratoire de Photonique et de Nanostructures, Route de Nozay 91460 Marcoussis, France*
(Dated: January 30, 2012)

Using a magnetic resonance force microscope (MRFM), the power emitted by a spin transfer nano-oscillator consisting of a normally magnetized Py|Cu|Py circular nanopillar is measured both in the autonomous and forced regimes. From the power behavior in the subcritical region of the autonomous dynamics, one obtains a quantitative measurement of the threshold current and of the noise level. Their field dependence directly yields both the spin torque efficiency acting on the thin layer and the nature of the mode which first auto-oscillates: the lowest energy, spatially most uniform spin-wave mode. From the MRFM behavior in the forced dynamics, it is then demonstrated that in order to phase-lock this auto-oscillating mode, the external source must have the same spatial symmetry as the mode profile, *i.e.*, a uniform microwave field must be used rather than a microwave current flowing through the nanopillar.

Recent progress in spin electronics have demonstrated that owing to the spin transfer torque (STT) [1, 2], biasing magnetic hybrid nanostructures by a direct current can lead to microwave emission. These spin transfer nano-oscillators (STNOs) [3–5] offer decisive advantages compared to existing technology in tunability, agility, compactness and integrability. In view of their applications in high-frequency technologies, a promising strategy to improve the coherence and increase the emitted microwave power of these devices is to mutually synchronize several of them [6–10].

The synchronization of the STNO oscillations to an external source has already been demonstrated [11, 12]. In particular, it has been shown that symmetric perturbations to the STNO trajectory favor even synchronization indices (ratio of the external frequency to the STNO frequency $r = 2, 4, 6...$), while antisymmetric perturbations favor odd synchronization indices [13, 14]. But so far, the influence of the spatial symmetry of the spin-wave (SW) mode which auto-oscillates on the synchronization rules has not been elucidated.

To address this open question, the spectroscopic identification of the auto-oscillating mode is crucial. It is usually a challenge, as a large variety of dynamic modes can be excited in STNOs, and their nature can change depending on the geometry, magnetic parameters and bias conditions. In this work, we study a STNO in the most simple configuration: a circular nanopillar saturated by a strong magnetic field applied along its normal. It corresponds to an optimum configuration for synchronization, since it has a maximal nonlinear frequency shift, which provides a large ability for the STNO to lock its phase to an external source [8]. Moreover, the perpendicular configuration coincides with the universal oscillator model, for which an exact analytical theory can be derived [15]. Last but not least, this highly symmetric case allows for a simplified classification of the SW eigenmodes inside the STNO [16].

We shall use here a magnetic resonance force microscope (MRFM) to monitor directly the power emitted by this archetype STNO vs. the bias dc current and perpendicular magnetic field. In the autonomous regime, these quantitative measurements allow us to demonstrate that the mode which auto-oscillates just above the threshold current is the fundamental, spatially most uniform SW mode. By studying the forced regime, we then show that this mode synchronizes only to an external source sharing the same spatial symmetry, namely, a uniform microwave magnetic field, and *not* the common microwave current passing through the device.

For this study, we use a circular nanopillar of nominal diameter 200 nm patterned from a $(Cu60|Py_B15|Cu10|Py_A4|Au25)$ stack, where thicknesses are in nm and $Py=Ni_{80}Fe_{20}$. A dc current I_{dc} and a microwave current i_{rf} can be injected through the STNO using the bottom Cu and top Au electrodes. A positive current corresponds to electrons flowing from the thick Py_B to the thin Py_A layer. This STNO device is insulated and an external antenna is patterned on top to generate a spatially uniform microwave magnetic field h_{rf} oriented in the plane of the magnetic layers. The bias magnetic field H_{ext}, ranging between 8.5 and 11 kOe, is applied at $\theta_H = 0°$ from the normal to the sample plane.

The room temperature MRFM setup [17] consists of a spherical magnetic probe attached at the end of a very soft cantilever, coupled dipolarly to the buried nanopillar (see inset of Fig.1) and positioned 1.5 μm above its center. This mechanical detection scheme [18, 19] sensitively measures the variation of the longitudinal magnetization ΔM_z over the whole volume of the magnetic body [20], a quantity *directly* proportional to the normalized power
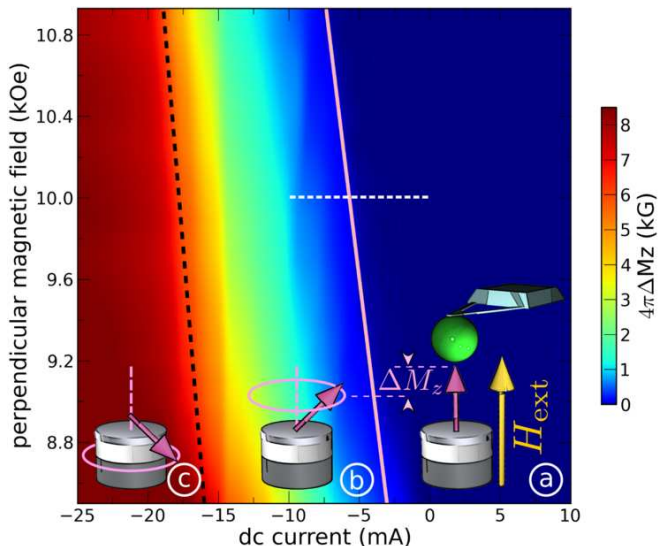
FIG. 1. (Color online). Phase diagram of the STNO autonomous dynamics measured by MRFM.

p emitted by the STNO [15]:

$$p = \frac{\Delta M_z}{2M_s},\qquad(1)$$

where M_s is the saturation magnetization of the precessing layer.

First, we measure the phase diagram of the STNO autonomous dynamics as a function of I_{dc} and H_{ext}, see Fig.1. In this experiment, I_{dc} is fully modulated at the cantilever frequency, $f_c \approx 12$ kHz, and the mechanical signal represents ΔM_z synchronous with the injection of I_{dc} through the STNO. This quantitative measurement [21] is displayed using the color scale indicated on the right of Fig.1.

Three different regions can be distinguished in this phase diagram. At low negative or positive current (region ⓐ), ΔM_z is negligible, because in the subcritical region, the STT is not sufficient to destabilize the magnetization in the thin or thick layer away from the perpendicular applied field direction. As I_{dc} is reaching a threshold negative value (from −3 to −7 mA as H_{ext} increases from 8.5 to 10.7 kOe, see pink solid line in Fig.1), the MRFM signal starts to smoothly increase in region ⓑ. It corresponds to the onset of spin transfer driven oscillations in the thin layer, which will be analyzed in details below. As I_{dc} is further decreased towards more negative values, the angle of precession increases in the thin layer, until it eventually reaches 90°: at the boundary between regions ⓑ and ⓒ (see black dashed line) $4\pi\Delta M_z$ equals the full saturation magnetization in the thin layer, $4\pi M_s = 8$ kG.

Let us now concentrate on the spin transfer dynamics in the thin layer at $I_{dc} < 0$. We first turn to the quantitative analysis of the subcritical region ⓐ. We introduce

$\mathcal{N} = VM_s/(g\mu_B)$, the number of spins in the thin layer (V is its volume, g the Landé factor, μ_B the Bohr magneton). The averaged normalized power p in the subcritical regime ($|I_{dc}| < I_{th}$) is evaluated in the stochastic nonlinear oscillator model described in section VII of ref. [15]. Under the assumption that only one SW mode dominates the STNO autonomous dynamics, Eq.(1) follows the simple relationship:

$$\frac{\Delta M_z}{2M_s} = \frac{k_B T}{\mathcal{N}\hbar\omega_\nu}\frac{1}{1-I_{dc}/I_{th}},\qquad(2)$$

where $I_{th} = 2\alpha\omega_\nu\mathcal{N}e/\epsilon$ is the threshold current for auto-oscillation of the SW mode ν with frequency ω_ν (α is the Gilbert damping constant in the thin layer, e the electron charge, and ϵ the spin torque efficiency). In Eq.(2), the prefactor

$$\eta \equiv \frac{k_B T}{\mathcal{N}\hbar\omega_\nu}\qquad(3)$$

is the noise power: the ratio between the thermal energy (k_B is the Boltzmann constant, T the temperature) and the maximal energy stored in the SW mode ν ($\hbar$ is the Planck constant over 2π).

From Eq.(2), the inverse power is linear with the bias current I_{dc} in the subcritical region. A sample measurement at $H_{ext} = 10$ kOe (along the white dashed line in Fig.1) is shown in Fig.2a. From a linear fit, one can thus obtain the threshold current I_{th} and the noise power η at this particular field. The dependencies of I_{th} and η on the perpendicular magnetic field are plotted in Figs.2b and 2c, respectively.

The parameters V, M_s, g (hence, $\mathcal{N} \simeq 6.3\times10^6$) and $\alpha = 0.014$ of the thin layer have been determined from an extensive MRFM spectroscopic study performed at $I_{dc} = 0$ on the same sample and published in ref.[16]. This study also yields the dispersion relations $\omega_\nu = \gamma(H_{ext} - H_\nu)$ of the thin layer SW modes ($\gamma = g\mu_B/\hbar = 1.87\times10^7$ rad.s⁻¹.G⁻¹ is the gyromagnetic ratio, H_ν the so-called Kittel field associated to the mode ν). By injecting ω_ν in the expression of the threshold current, it is found that the latter depends linearly on the perpendicular bias field:

$$I_{th} = \frac{2\alpha\mathcal{N}e}{\epsilon}\gamma(H_{ext} - H_\nu),\qquad(4)$$

as observed in Fig.2b. The linear fit of I_{th} vs. H_{ext} using Eq.(4) yields $H_\nu = 6.80 \pm 0.15$ kOe and $\epsilon = 0.30 \pm 0.005$. The importance of the analysis of Fig.2b is that, first, it provides an accurate determination of the spin torque efficiency, found to be in agreement with the accepted value in similar STNO stacks [22]. Second, a comparison with the SW modes of the thin layer (see black symbols extracted from ref.[16] and mode profiles in Fig.2b) shows that the fitted value of H_ν precisely corresponds to the Kittel field of the $(\ell,n) = (0,0)$ mode, ℓ and n being respectively the azimuthal and radial mode indices. It thus
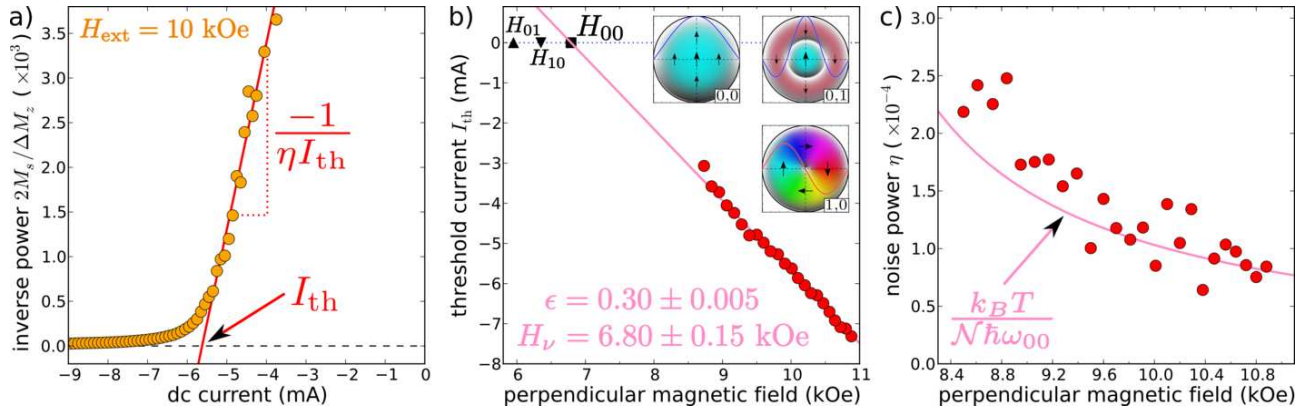
FIG. 2. (Color online). (a) Determination of the threshold current I_{th} and noise power η at H_{ext} = 10 kOe, from the inverse MRFM signal in the subcritical regime. Dependencies of the threshold current (b) and noise power (c) on the perpendicular magnetic field.

allows us to conclude about the nature of the mode that first auto-oscillates at $I_{\text{dc}} < 0$ as being the fundamental, most uniform precession mode of the thin layer.

To gain further insight in our analysis of the subcritical regime, we compare in Fig.2c the noise power determined as a function of H_{ext} with the prediction of Eq.(3), in which the dispersion relation of the $\nu = (0,0)$ SW mode is used. It is found that the fluctuations of the STNO power are well accounted for by those of the previously identified auto-oscillating mode, which confirms that the single mode assumption made to derive Eq.(2) is a good approximation.

Using two different microwave circuits, we shall now compare the ability of the auto-oscillating SW mode to phase-lock either to the uniform microwave field h_{rf} generated by the external antenna, or to the microwave current i_{rf} flowing through the nanopillar. We know from previous studies that in the exact perpendicular configuration, the SW spectrum critically depends on the method of excitation [16]: h_{rf} excites only the axially symmetric modes having azimuthal index $\ell = 0$, whereas due to the orthoradial symmetry of the induced microwave Oersted field, i_{rf} excites only the modes having azimuthal index $\ell = +1$. The dependencies on I_{dc} and H_{ext} of the STNO dynamics forced respectively by h_{rf} and i_{rf} are presented in Figs.3a and 3b. The plotted quantity is ΔM_z synchronous with the full modulation of the external source power: h_{rf} = 1.9 Oe (a) and i_{rf} = 140 μA (b). Although the $\ell = 0$ and $\ell = +1$ spectra are in principle shifted by 1.1 GHz from each other, a direct comparison of the phase diagrams (a) and (b) can be made by using different excitation frequencies for h_{rf} (8.1 GHz) and i_{rf} (9.2 GHz).

Below the threshold current (indicated by the pink lines in Fig.3), the observed behaviors of the $\ell = 0$ and $\ell = +1$ modes are alike: a small negative dc current slightly attenuates the SW modes $B_{\ell n}$ of the thick Py_B layer, while it promotes quite rapidly the SW modes $A_{\ell n}$
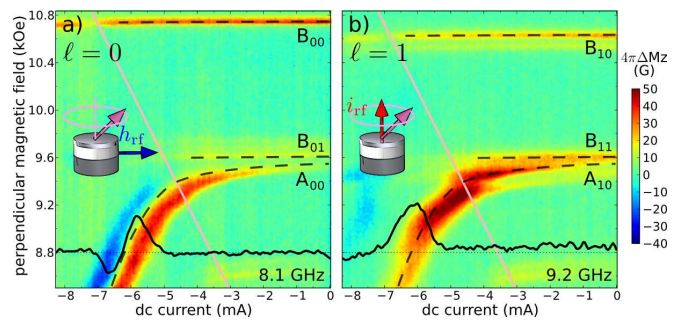

FIG. 3. (Color online). MRFM measurement of the STNO dynamics forced by (a) the uniform field h_{rf} at 8.1 GHz and (b) the orthoradial Oersted field produced by i_{rf} at 9.2 GHz, as a function of I_{dc} and H_{ext}. The black traces show the MRFM signal vs. I_{dc} at H_{ext} = 8.8 kOe. The pink solid lines show the location of the threshold current determined in Fig.2b. The dashed lines are guides to the eye.

of the thin Py_A layer, in agreement with the expected symmetry of the STT [16]. On the contrary, there is a clear qualitative difference between the modes A_{00} and A_{10} beyond I_{th}. Although both peaks similarly shift towards lower field as I_{dc} is decreased towards lower negative values, A_{00} gets strongly distorted, with the appearance of a negative dip on its high field side, in contrast to A_{10}, which remains a positive peak.

The negative MRFM signal observed in Fig.3a in the region of spin transfer driven oscillations in the thin layer is striking, because it means that the precession angle can be *reduced* in the presence of the microwave excitation h_{rf}. As a matter of fact, the distortion of the peak A_{00} is associated to the synchronization of the auto-oscillating mode to the external signal. Fig.4a illustrates the distortion of the STNO emission frequency induced by this phenomenon. These data were obtained by monitoring the fluctuating voltage across the nanopillar at I_{dc} = −7 mA with a spectrum analyzer as a function of
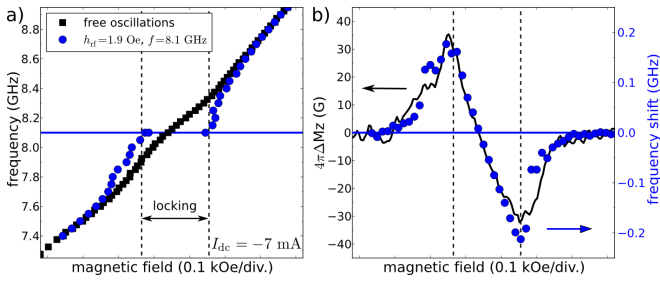
FIG. 4. (Color online). (a) Magnetic field dependence of the STNO frequency in the free and forced regimes (the external source at 8.1 GHz is h_{rf}). (b) Comparison between the STNO frequency shift deduced from (a) and the MRFM signal.

phase-lock the STNO dynamics in the present work. We believe that this finding might be important for future strategies to synchronize large STNOs arrays.

the applied magnetic field [23]. The frequency shift of the forced oscillations with respect to the free running oscillations is plotted in Fig.4b, along with the MRFM signal. This demonstrates that in the so-called phase-locking range, the STNO amplitude adapts ($\Delta M_z > 0$: increases, $\Delta M_z < 0$: decreases), so as to maintain its frequency equal to the frequency of the source, here fixed at 8.1 GHz. This comparison also allows to estimate the phase-locking bandwidth, found to be as large as 0.4 GHz despite the small amplitude of the external signal. The nonlinear frequency shift is indeed the largest in the perpendicular configuration, $N = 4\gamma M_s \simeq 48$ GHz [15], therefore, a small change of the power emitted by the STNO is sufficient to change its frequency by a substantial amount.

Such a signature of synchronization of the auto-oscillating mode is not observed in Fig.3b, where the external source is the microwave current. This highlights the crucial importance of the symmetry associated to the SW mode driven by STT: in the exact perpendicular configuration, i_{rf} can only excite $\ell = +1$ SW modes, therefore, it has the wrong symmetry to couple to the auto-oscillating mode, which was shown in Fig.2 to bare the azimuthal index $\ell = 0$. We add that in our exact axially symmetrical case, no phase-locking behavior is observed with the even synchronization index $r = 2$, neither with i_{rf}, nor with h_{rf}, which is due to the perfectly circular STNO trajectory.

To conclude, based on the quantitative analysis of both the critical current and the noise power in the subcritical regime, we have unambiguously identified the auto-oscillating mode in the perpendicular configuration of a nanopillar. This case is particularly interesting due to its large ability to synchronize to an external source. But we have shown that in addition to the symmetry of the perturbation with respect to the STNO trajectory [14], the overlap integral between the external source and the auto-oscillating mode profile is crucial to synchronization rules. Due to symmetry reasons, only the uniform microwave field applied perpendicularly to the bias field and with the synchronization index $r = 1$ is efficient to

* Corresponding author: gregoire.deloubens@cea.fr
† Co-author: olivier.klein@cea.fr
[1] J. Slonczewski, J. Magn. Magn. Mater. **159**, L1 (1996).
[2] L. Berger, Phys. Rev. B **54**, 9353 (1996).
[3] S. I. Kiselev, J. C. Sankey, I. N. Krivorotov, N. C. Emley, R. J. Schoelkopf, R. A. Buhrman, and D. C. Ralph, Nature **425**, 380 (2003).
[4] W. H. Rippard, M. R. Pufall, S. Kaka, S. E. Russek, and T. J. Silva, Phys. Rev. Lett. **92**, 027201 (2004).
[5] D. Houssameddine, U. Ebels, B. Delat, B. Rodmacq, I. Firastrau, F. Ponthenier, M. Brunet, C. Thirion, J.-P. Michel, L. Prejbeanu-Buda, M.-C. Cyrille, O. Redon, and B. Dieny, Nature Mater. **6**, 447 (2007).
[6] S. Kaka, M. R. Pufall, W. H. Rippard, T. J. Silva, S. E. Russek, and J. A. Katine, Nature **437**, 389 (2005).
[7] F. B. Mancoff, N. D. Rizzo, B. N. Engel, and S. Tehrani, Nature **437**, 393 (2005).
[8] A. N. Slavin and V. S. Tiberkevich, Phys. Rev. B **72**, 092407 (2005).
[9] J. Grollier, V. Cros, and A. Fert, Phys. Rev. B **73**, 060409 (2006).
[10] A. Ruotolo, V. Cros, B. Georges, A. Dussaux, J. Grollier, C. Deranlot, R. Guillemet, K. Bouzehouane, S. Fusil, and A. Fert, Nature Nanotech. **4**, 528 (2009).
[11] W. H. Rippard, M. R. Pufall, S. Kaka, T. J. Silva, S. E. Russek, and J. A. Katine, Phys. Rev. Lett. **95**, 067203 (2005).
[12] B. Georges, J. Grollier, M. Darques, V. Cros, C. Deranlot, B. Marcilhac, G. Faini, and A. Fert, Phys. Rev. Lett. **101**, 017201 (2008).
[13] M. Quinsat, J. F. Sierra, I. Firastrau, V. Tiberkevich, A. Slavin, D. Gusakova, L. D. Buda-Prejbeanu, M. Zarudniev, J.-P. Michel, U. Ebels, B. Dieny, M.-C. Cyrille, J. A. Katine, D. Mauri, and A. Zeltser, Appl. Phys. Lett. **98**, 182503 (2011).
[14] S. Urazhdin, P. Tabor, V. Tiberkevich, and A. Slavin, Phys. Rev. Lett. **105**, 104101 (2010).
[15] A. Slavin and V. Tiberkevich, IEEE Trans. Magn. **45**, 1875 (2009).
[16] V. V. Naletov, G. de Loubens, G. Albuquerque, S. Borlenghi, V. Cros, G. Faini, J. Grollier, H. Hurdequint, N. Locatelli, B. Pigeau, A. N. Slavin, V. S. Tiberkevich, C. Ulysse, T. Valet, and O. Klein, Phys. Rev. B **84**, 224423 (2011).
[17] O. Klein, G. de Loubens, V. V. Naletov, F. Boust, T. Guillet, H. Hurdequint, A. Leksikov, A. N. Slavin, V. S. Tiberkevich, and N. Vukadinovic, Phys. Rev. B **78**, 144410 (2008).
[18] G. de Loubens, V. V. Naletov, O. Klein, J. Ben Youssef, F. Boust, and N. Vukadinovic, Phys. Rev. Lett. **98**, 127601 (2007).

[19] B. Pigeau, G. de Loubens, O. Klein, A. Riegler, F. Lochner, G. Schmidt, and L. W. Molenkamp, Nature Phys. **7**, 26 (2011).

[20] G. de Loubens, V. V. Naletov, and O. Klein, Phys. Rev. B **71**, 180411 (2005).

[21] V. V. Naletov, V. Charbois, O. Klein, and C. Fermon, Appl. Phys. Lett. **83**, 3132 (2003).

[22] V. S. Rychkov, S. Borlenghi, H. Jaffres, A. Fert, and X. Waintal, Phys. Rev. Lett. **103**, 066602 (2009).

[23] Here, a slight tilt of the angle $\theta_H = 2°$ is required. Indeed, no oscillatory voltage is produced in the exact perpendicular configuration, due to the perfect axial symmetry of the STNO trajectory.